

Universal Spin-Hall Conductance Fluctuations in Two Dimensions

Wei Ren,¹ Zhenhua Qiao,¹ Jian Wang,^{2,*} Qingfeng Sun,³ and Hong Guo⁴

¹*Department of Physics, The University of Hong Kong, Hong Kong, China*

²*Department of Physics and the Center of Theoretical and Computational Physics, The University of Hong Kong, Hong Kong, China*

³*Beijing National Laboratory for Condensed Matter Physics and Institute of Physics, Chinese Academy of Sciences, Beijing 100080, China*

⁴*Department of Physics, McGill University, Montreal, Quebec, Canada*

(Received 13 January 2006; published 11 August 2006)

We report a theoretical investigation on spin-Hall conductance fluctuation of disordered four-terminal devices in the presence of Rashba or/and Dresselhaus spin-orbital interactions in two dimensions. As a function of disorder, the spin-Hall conductance G_{SH} shows ballistic, diffusive, and insulating transport regimes. For given spin-orbit interactions, a universal spin-Hall conductance fluctuation (USCF) is found in the diffusive regime. The value of the USCF depends on the spin-orbit coupling t_{so} but is independent of other system parameters. It is also independent of whether Rashba or Dresselhaus or both spin-orbital interactions are present. When t_{so} is comparable to the hopping energy t , the USCF is a universal number $\sim 0.18e/4\pi$. The distribution of G_{SH} crosses over from a Gaussian distribution in the metallic regime to a non-Gaussian distribution in the insulating regime as the disorder strength is increased.

DOI: [10.1103/PhysRevLett.97.066603](https://doi.org/10.1103/PhysRevLett.97.066603)

PACS numbers: 72.25.-b, 71.70.Ej, 72.15.Rn

The notion of a dissipationless spin current [1] has attracted considerable interest recently. In its simplest form, a spin current is about the flow of spin-up electrons in one direction, say, $+x$, accompanied by the flow of an equal number of spin-down electrons in the opposite direction, $-x$. The total charge current in the x direction is therefore zero, $I_e = e(I_{\uparrow} + I_{\downarrow}) = 0$; and the total spin current is finite: $I_s = \hbar/2(I_{\uparrow} - I_{\downarrow}) \neq 0$. For a pure semiconductor system with spin-orbital (SO) interactions, it has been shown [1] that an electric field in the z direction can induce the flow of a spin current in the x direction perpendicular to the electric field: such a spin current is dissipationless because the external electric field does no work to the electrons flowing inside the spin current. If the semiconductor sample has a finite x extent, the flow of spin current should cause a spin accumulation at the edges of the sample, resulting in a situation where spin-up electrons accumulate at one edge while spin-down electrons accumulate at the opposite edge. Hence a spin-Hall effect [2,3] is produced where chemical potentials for the two spin channels become different at the two edges of the sample. This interesting phenomenon has been subjected to extensive studies, and there are several experiments reporting spin accumulation which may have provided evidence of this effect [4]. It has been shown that for a pure two-dimensional sample without any impurities, the Rashba SO interaction generates a spin-Hall conductivity having a universal value of $e/8\pi$ [3]. It has also been shown that any presence of weak disorder destroys this spin-Hall effect in the large sample limit [5,6]. On the other hand, numerical studies have provided evidence that for mesoscopic samples, spin-Hall conductance can survive weak disorder [7–9].

One of the most striking quantum transport features in the mesoscopic regime is the universal charge conductance

fluctuation (UCF) [10–12]: quantum interference gives rise to the sample-to-sample fluctuation of charge conductance of order e^2/h , independent of the details of the disorder, Fermi energy, and the sample size as long as transport is in the coherent diffusive regime characterized by the relation between relevant length scales, $l < L < \xi$. Here L is the linear sample size, l the elastic mean free path, and ξ the phase coherence length. If time-reversal symmetry is broken, UCF is suppressed by a factor of 2.

A very important and interesting issue therefore arises: What are the properties of the fluctuations of *spin-Hall conductance* in disordered samples? Is there a transport regime where spin-Hall conductance fluctuation is *universal*? The answers to these questions are nontrivial because the flow of dissipationless spin current is qualitatively different from the flow of charge current driven by an external electric field. It is the purpose of this Letter to report our investigations of these issues. For a disordered four-terminal sample with a given Rashba SO interaction strength t_{so} , and/or Dresselhaus interaction strength $t_{\text{so}2}$, our results suggest that there is indeed a universal spin-Hall conductance fluctuation (USCF) whose root mean square amplitude is $g = 0.18(e/4\pi)$, independent of other system details (thus universal). The fluctuation is, however, a function of the SO interaction strength and found to be well fitted by a functional form of $\text{rms}(G_{\text{SH}}) = g \tanh(|t_{\text{so}} - t_{\text{so}2}|/0.17)$. Finally, the distribution of spin-Hall conductance obeys a Gaussian distribution in the metallic regime and deviates from it in the insulating regime.

To investigate USCF, we consider a four-terminal device in two-dimensions schematically shown in the left inset of Fig. 1. We will first discuss the results in the presence of only Rashba interaction. In the presence of Rashba interaction [$\alpha_{\text{so}}\mathbf{z} \cdot (\boldsymbol{\sigma} \times \mathbf{k})$], the Hamiltonian of this device is given by [8]

$$H = -t \sum_{\langle ij \rangle \sigma} (c_{i\sigma}^\dagger c_{j\sigma} + \text{H.c.}) - t_{\text{so}} \sum_i [(c_{i\uparrow}^\dagger c_{i+\hat{x},\downarrow} - c_{i\downarrow}^\dagger c_{i+\hat{x},\uparrow}) - i(c_{i\uparrow}^\dagger c_{i+\hat{y},\downarrow} + c_{i\downarrow}^\dagger c_{i+\hat{y},\uparrow}) + \text{H.c.}] + \sum_{i\sigma} \epsilon_i c_{i\sigma}^\dagger c_{i\sigma}, \quad (1)$$

where $c_{i\sigma}^\dagger$ is the creation operator for an electron with spin σ on site i , and \hat{x} and \hat{y} are unit vectors along the x and y directions. Here $t = \hbar^2/2ma^2$ is the hopping energy and $t_{\text{so}} = \alpha_{\text{so}}/2a$ is the effective spin-orbit coupling. The on-site energy is given by $\epsilon_i = 4t$. In addition, static Anderson-type disorder is added to ϵ_i with a uniform distribution in the interval $[-W/2, W/2]$, where W characterizes the strength of the disorder. We consider the situation where Rashba interaction is present everywhere except in leads 2 and 4 (see the left inset of Fig. 1) in order to measure the conserved spin current [8]. We apply external bias voltages at the four terminals as $(V_i, i = 1, \dots, 4) = (v/2, 0, -v/2, 0)$: such a setup generates a spin current flowing from lead 2 to 4, i.e., a spin-Hall effect measured from these two leads [8].

The spin-Hall conductance G_{SH} is calculated from the Landauer-Buttiker formula [7]:

$$G_{\text{SH}} = (e/8\pi)[(T_{2\uparrow,1} - T_{2\downarrow,1}) - (T_{2\uparrow,3} - T_{2\downarrow,3})], \quad (2)$$

where the transmission coefficient is given by $T_{2\sigma,1} = \text{Tr}(\Gamma_{2\sigma} G^r \Gamma_1 G^a)$; here $G^{r,a}$ are the retarded and advanced Green functions of the central disordered region of the device which we evaluate numerically. The quantities $\Gamma_{i\sigma}$

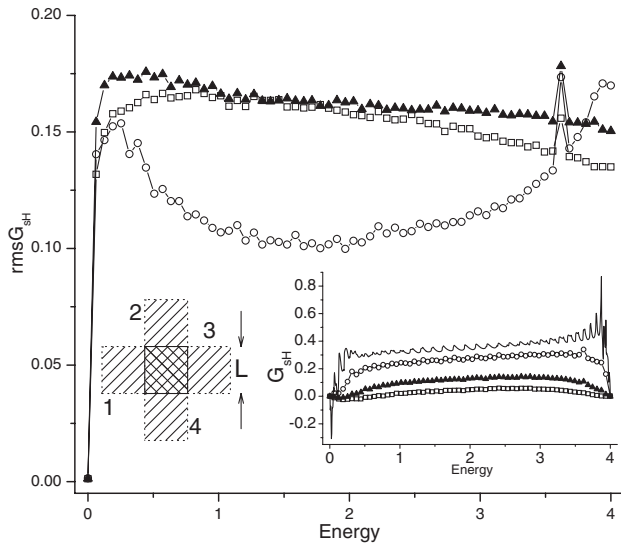


FIG. 1. Spin-Hall conductance fluctuation vs energy for disordered samples. Triangles, squares, and circles are for $W = 1, 2, 3$, respectively. Left inset: schematic plot of the four-terminal mesoscopic sample where Rashba interaction exists in the center scattering region and the leads 1,3. The width of the square sample is L . A small voltage bias is across leads 1,3, and spin-Hall conductance is measured through leads 2,4. Right inset: the ensemble averaged spin-Hall conductance G_{SH} vs electron energy for SO interaction strength $t_{\text{so}} = 0.3$. Solid line, pure sample with $W = 0$; other symbols are the same as the main panel. In all figures the spin conductance and its fluctuation are measured in $e/4\pi$.

are the line width functions describing coupling of the leads to the scattering region, and are obtained by calculating self-energies due to the semi-infinite leads using a transfer matrices method [13]. The spin-Hall conductance fluctuation is defined as $\text{rms}(G_{\text{SH}}) \equiv \sqrt{\langle G_{\text{SH}}^2 \rangle - \langle G_{\text{SH}} \rangle^2}$, where $\langle \dots \rangle$ denotes averaging over an ensemble of samples with different configurations of the same disorder strength W . Note that in the presence of disorder, although one could use another definition $\bar{G}_{\text{SH}} = (e/4\pi) \times (T_{2\uparrow,1} - T_{2\downarrow,1})$ to calculate and obtain the same average spin-Hall conductance as that of G_{SH} , the spin-Hall fluctuation can only be obtained correctly using the definition of Eq. (2). We perform our calculations on $L \times L$ square samples with four leads described above. Sample sizes of $L = 40$ up to 100 are examined [14]. To fix units, throughout this Letter we measure the energy E , disorder strength W , and spin-orbit coupling t_{so} in terms of the hopping matrix t .

Figure 1 plots spin-Hall conductance fluctuation vs Fermi energy at a fixed $t_{\text{so}} = 0.3$ and sample size $L = 40$ for several disorder strengths $W = 1, 2, 3$. We have also shown the averaged spin-Hall conductance in the right inset. Because of the electron/hole symmetry, only data for energy range $[0, 4]$ are shown. Over 10 000 disordered samples are averaged. For pure sample without disorder, as the Fermi energy is increased, the number of subbands increase. As a result, the spin-Hall conductance G_{SH} shows small oscillations. When disorder is increased from zero, G_{SH} decreases as expected, and eventually the small oscillation due to the subbands vanishes. Most importantly, Fig. 1 shows substantial sample-to-sample fluctuations of G_{SH} , measured by $\text{rms}(G_{\text{SH}})$, of the order $\delta \frac{e}{4\pi}$, where δ is a number between 0.1 and 0.2. Such an amplitude of fluctuation is comparable to the spin-Hall conductance itself.

In Figs. 2(a) and 2(b), we plot the $\langle G_{\text{SH}} \rangle$ and $\text{rms}(G_{\text{SH}})$ as a function of disorder strength W at fixed Fermi energy $E = 1$ for a number of different spin-orbit couplings from $t_{\text{so}} = 0.2$ up to 0.7. Several observations are in order. First, the spin-Hall conductance [Fig. 2(a)] decreases smoothly as the disorder strength is increased: the transport characteristics goes from quasiballistic at small W to the diffusive regime at larger W . In the diffusive regime, the spin-Hall conductance decreases exponentially with the disorder strength between $W = [1, 5]$. Finally it goes to the insulating regime for even larger W where G_{SH} vanishes. Second, the numerical data show that the onsets of insulating regime W_c are different for different spin-orbit couplings t_{so} . The larger the spin-orbit coupling, the larger W_c . This finding is consistent with that of Ref. [8], which suggested that the localization length depends on t_{so} and belongs to two-parameter scaling. Third, from the spin-Hall conductance fluctuation shown in Fig. 2(b), we observe that for small disorder $W < 1$, the fluctuations for different t_{so} have

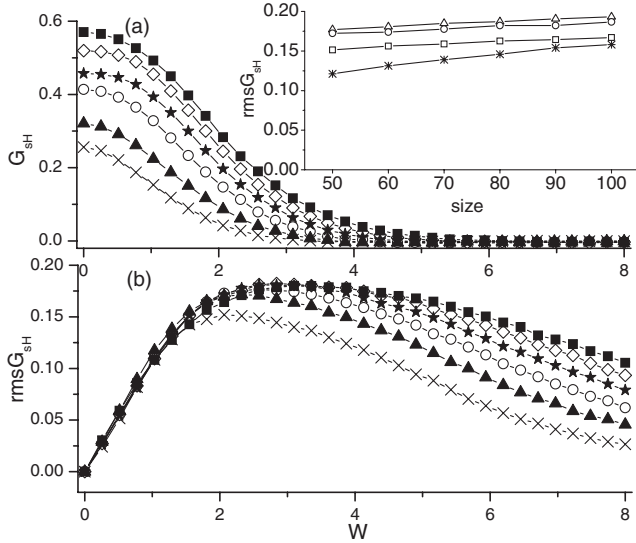


FIG. 2. (a) Ensemble averaged G_{SH} vs disorder strength W for $t_{\text{SO}} = 0.2$ (cross), 0.3 (solid triangle), 0.4 (open circle), 0.5 (star), 0.6 (rumbus), and 0.7 (solid square). The average is over 20 000 samples with $L = 40$. Inset: size dependence of spin-Hall conductance fluctuation with $t_{\text{SO}} = 0.3$. Different symbols are for $W = 1$ (stars), 2 (rectangles), 3 (circles), and 4 (triangles). The ensemble average is over 20 000 samples for different size L . (b) The corresponding ensemble averaged spin-Hall conductance fluctuation vs W ; the symbols are for the same t_{SO} values as in (a).

very similar values and the curves collapse. For larger disorder, the fluctuations develop a plateau structure so that $\text{rms}(G_{\text{SH}})$ becomes independent of the disorder parameter W for each given t_{SO} . In this sense, the fluctuation $\text{rms}(G_{\text{SH}})$ becomes “universal” and the spin-Hall transport enters the regime with USCFs. Importantly, both the width of the plateau and the value of USCF depend on t_{SO} . The larger the t_{SO} , the wider the fluctuation plateau which characterizes the diffusive regime.

Now we examine the dependence of spin-Hall conductance fluctuation $\text{rms}(G_{\text{SH}})$ on system size L in the inset of Fig. 2(a) for $t_{\text{SO}} = 0.3$. With weak disorder $W = 1$ (stars) the fluctuation increases with sample size indicating that spin-Hall conductance is not yet in the USCF regime because transport is quasiballistic. In the diffusive regime, $W = 2, 3, 4$, the fluctuations saturate at $\delta e/4\pi$ where $\delta \approx 0.2$. The independence of system size by the fluctuation $\text{rms}(G_{\text{SH}})$ provides strong evidence of USCF. Namely, as long as transport is in the diffusive regime, the fluctuation of the spin-Hall conductance is dominated by quantum interference giving rise to a universal amplitude. Since the value of USCF [which is obtained from each curve in Fig. 2(b)] depends on the spin-orbit coupling t_{SO} as seen from Fig. 2, we have obtained a collection of the USCF for different t_{SO} which is shown in Fig. 3(a). Interestingly, the USCF can be well fitted (solid line) by a function $\text{rms}(G_{\text{SH}}) = g \tanh(t_{\text{SO}}/0.17)$, where $g = 0.18e/4\pi$. This can be understood as follows. When $t_{\text{SO}} = 0$, there is no spin-Hall current and hence no fluctuations. There is a

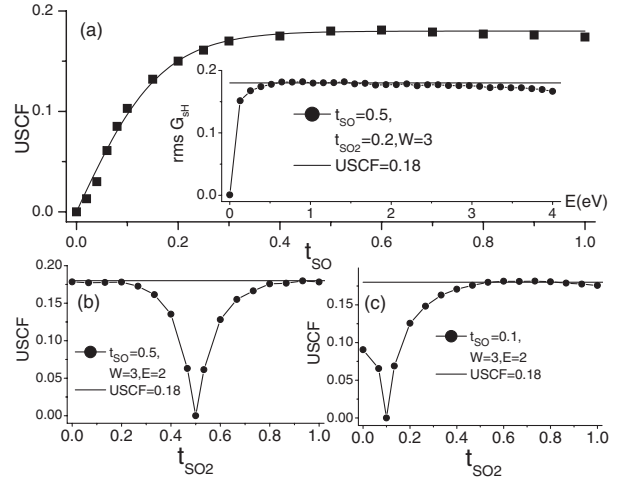


FIG. 3. (a) USCF values vs Rashba spin-orbit coupling t_{SO} at $E = 1$. Inset: $\text{rms}G_{\text{SH}}$ vs Fermi energy for $W = 3$ in the presence of both Rashba and Dresselhaus SO coupling, $t_{\text{SO}} = 0.5$ and $t_{\text{SO}2} = 0.2$. (b), (c) $\text{rms}G_{\text{SH}}$ vs Dresselhaus SO coupling $t_{\text{SO}2}$ at $E = 2$, $W = 3$, and $t_{\text{SO}} = 0.5/t_{\text{SO}2} = 0.1$. In the cases of inset of (a), (b), and (c), 40 000 samples are collected.

crossover regime before the fluctuation saturates to the USCF plateau.

Figures 4(a)–4(d) plot the distribution function of spin-Hall conductance, $P(G_{\text{SH}})$, for several different disorder values W . For each W , data are accumulated by calculating 20 000 realizations of disorder. $P(G_{\text{SH}})$ appears to clearly obey a Gaussian distribution in the metallic regime up to $W \approx 5$. For larger W between [5, 10], transport is in the insulating regime; the symmetric distribution exhibits non-Gaussian behavior [Fig. 4(c)]. At even larger disorder $W = 12$ shown in Fig. 4(d), the distribution becomes non-Gaussian and asymmetric. The deviation from Gaussian distribution can be characterized by the moments of spin-Hall conductance. We have calculated the skewness γ_1 and kurtosis γ_2 whose definitions are [15] $\gamma_1 = \mu_3/\mu_2^{3/2}$ and $\gamma_2 = \mu_4/\mu_2^2 - 3$, where $\mu_n = \langle (x - \langle x \rangle)^n \rangle$ ($n = 2, 3, 4$) denote the central moments. The skewness describes the degree of asymmetry of a distribution around its mean, while the kurtosis measures the relative peakedness of a distribution. The results are plotted in Fig. 4(f), showing that in the metallic regime $W < 5$, both skewness and kurtosis are essentially zero while they become nonzero for larger W , consistent with the distributions. Hence the skewness and kurtosis can be used to identify the diffusive regime. Importantly, these quantities can be measured experimentally [10]. Finally, we have checked that the above features of the spin-Hall conductance fluctuation are generic and valid for other values of E and t_{SO} . For instance, Fig. 4(f) shows the $\text{rms}G_{\text{SH}}$ vs Fermi energy when $W = 3$ and $t_{\text{SO}} = 0.6, 0.7$. We see that between $E = 1$ and $E = 3$, $\text{rms}G_{\text{SH}}$ is around the universal value 0.18.

So far we have focused on spin-Hall conductance fluctuations with the Rashba interaction. To further demonstrate the universal behavior, we have also analyzed the

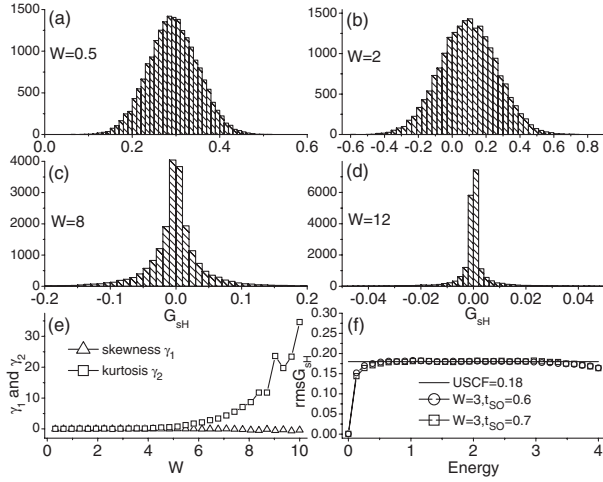


FIG. 4. (a)–(d) The distribution of the spin-Hall conductance for different disorder strengths at a fixed energy $E = 1$ and $t_{\text{SO}} = 0.3$. Data are collected for 20 000 samples for each W with $L = 40$. (e) The skewness γ_1 and kurtosis γ_2 vs disorder strength W for the same ensemble. (f) $\text{rms}G_{\text{SH}}$ vs Fermi energy for $W = 3$ and $t_{\text{SO}} = 0.6, 0.7$.

case of Dresselhaus spin-orbital interaction by adding a term $\beta_{\text{so}}(\sigma_x k_x - \sigma_y k_y)$ in Eq. (1). Using unitary transformations, it is easy to prove that for the spin-Hall current along the z direction we have $I_{\text{SH}}^z(\alpha_{\text{so}} = 0, \beta_{\text{so}}) = I_{\text{SH}}^z(\alpha_{\text{so}}, \beta_{\text{so}} = 0)$ and $I_{\text{SH}}^z(\alpha_{\text{so}} = \beta_{\text{so}}) = 0$. When there is no Rashba spin-orbital interaction ($\alpha_{\text{so}} = 0$) and only Dresselhaus term exists, we have obtained exactly the same USC value and behavior as that of Rashba term alone. When both Rashba and Dresselhaus terms are present, it is not obvious that the USC persists. This is because these two terms have different symmetry—the Rashba coupling arises from the structure inversion asymmetry with $SU(2)$ symmetry, while the Dresselhaus coupling arises from the bulk inversion asymmetry with $SU(1,1)$ symmetry [16]. From Figs. 3(b) and 3(c) we see that for the latter situation (both α_{so} and $\beta_{\text{so}} \neq 0$), the results are similar to the case of pure Rashba or pure Dresselhaus interaction. Because $I_{\text{SH}}^z(\alpha_{\text{so}} = \beta_{\text{so}}) = 0$, the USC curves have a dip to zero when $\alpha_{\text{so}} = \beta_{\text{so}}$. Defining $t_{\text{SO}2} \equiv \beta_{\text{so}}/2a$, Figs. 3(b) and 3(c) show that USC is reached when $|t_{\text{SO}2} - t_{\text{SO}}| \sim 0.4$. Finally, the inset of Fig. 3(a) shows that the USC is independent of Fermi energy when both SO interactions are present.

In summary, for the spin-Hall effect generated by the Rashba and Dresselhaus interactions in mesoscopic samples, our results strongly suggest the existence of a universal spin-Hall conductance fluctuation due to impurity scattering in the quantum coherent regime. In this regime, the USC is characterized by sample-to-sample fluctuations of G_{SH} for a given SO interaction (Rashba or Dresselhaus) strength t_{SO} , measured by quantity $\text{rms}(G_{\text{SH}})$ with a universal amplitude $g \equiv \delta \frac{e}{4\pi}$ where $\delta \approx 0.18$, which is independent of system size, impurity scat-

tering strength, and Fermi energy. Importantly, this fluctuation amplitude is of the same order as the spin-Hall conductance itself. Comparing with the familiar UCF in charge conductance of disordered mesoscopic samples, USC originates from a similar physics of the quantum interference effect which leads to significant sample-to-sample fluctuations in spin-Hall conductance. A main difference is that the spin-Hall effect is due to SO interactions in the sample, thereby the USC also depends on the SO parameter t_{SO} (or $t_{\text{SO}2}$), and our numerical results can be well fitted by a functional form of $\text{rms}(G_{\text{SH}}) = g \tanh(|t_{\text{SO}} - t_{\text{SO}2}|/0.17)$.

This work was financially supported by a RGC grant (No. HKU 7044/05P) from the government SAR of Hong Kong. Q. F. S. is supported by NSF-China under Grants No. 90303016 and No. 10474125, and H. G. is supported by NSERC of Canada, FQRNT of Québec, and the Canadian Institute of Advanced Research. The Computer Centre of The University of Hong Kong is gratefully acknowledged for the high-performance computing assistance.

*Corresponding author.

- [1] S. Murakami *et al.*, *Science* **301**, 1348 (2003).
- [2] J. E. Hirsch, *Phys. Rev. Lett.* **83**, 1834 (1999).
- [3] J. Sinova *et al.*, *Phys. Rev. Lett.* **92**, 126603 (2004).
- [4] Y. K. Kato, R. C. Myers, A. C. Gossard, and D. D. Awschalom, *Science* **306**, 1910 (2004); J. Wunderlich, B. Kaestner, J. Sinova, and T. Jungwirth, *Phys. Rev. Lett.* **94**, 047204 (2005).
- [5] J. Inoue *et al.*, *Phys. Rev. B* **70**, 041303 (2004).
- [6] E. G. Mishchenko *et al.*, *Phys. Rev. Lett.* **93**, 226602 (2004).
- [7] E. M. Hankiewicz *et al.*, *Phys. Rev. B* **70**, 241301 (2004).
- [8] L. Sheng, D. H. Sheng, and C. S. Ting, *Phys. Rev. Lett.* **94**, 016602 (2005).
- [9] B. K. Nikolic *et al.*, *Phys. Rev. B* **72**, 075361 (2005).
- [10] S. Washburn and R. A. Webb, *Adv. Phys.* **35**, 375 (1986).
- [11] B. L. Altshuler, *Pis'ma Zh. Eksp. Teor. Fiz.* **41**, 530 (1985) [*JETP Lett.* **41**, 648 (1985)].
- [12] P. A. Lee and A. D. Stone, *Phys. Rev. Lett.* **55**, 1622 (1985).
- [13] M. P. López-Sancho, J. M. López-Sancho, and J. Rubio, *J. Phys. F* **14**, 1205 (1984); **15**, 851 (1985).
- [14] Because of the extremely large computational demands for adequate ensemble averaging, very careful coding must be done to exploit the mathematical structure of the self-energy and Hamiltonian matrices which allows the Green function to be obtained by inverting a tridiagonal matrix. For $L = 40$, our code takes approximately 10 min to calculate a curve of spin-Hall conductance vs energy with 200 energy points on a single personal computer. As tests, we have reproduced results in Figs. 1–3 of Ref. [8].
- [15] P. Mohanty *et al.*, *Phys. Rev. Lett.* **93**, 159702 (2004).
- [16] J. Schliemann, J. C. Egues, and D. Loss, *Phys. Rev. B* **67**, 085302 (2003).